Non-Linear model reduction for the Navier-Stokes Equations using the residual DEIM method

D. Xiao[a,b], F. Fang[a], A.G. Buchan[a], C.C. Pain[a], I.M. Navon[c,*], J. Du[d], G. Hu[b]

[a] *Applied Modelling and Computation Group, Department of Earth Science and Engineering,Imperial College London, Prince Consort Road, London, SW7 2BP, UK. URL:* `http://amcg.ese.imperial.ac.uk`

[b] *State Key Laboratory of Geological Processes and Mineral Resources, China University of Geosciences, Wuhan, 430074, China*

[c] *Department of Scientific Computing, Florida State University,Tallahassee, FL, 32306-4120, USA*

[d] *Institute of Atmospheric Physics, Chinese Academy of Sciences, Beijing, 100029, China*

1. Abstract

This article presents a new reduced order model based upon proper orthogonal decomposition (POD) for solving the Navier-Stokes equations. The novelty of the method lies in its treatment of the equation's non-linear operator, for which a new method is proposed that provides accurate simulations within an efficient framework. The method itself is a hybrid of two existing approaches that have already been developed to treat non-linear operators within reduced order models. The first of these approaches is one that approximates non-linear operators through quadratic expansions, and this is then blended within a second technique known as the Discrete Empirical Interpolation Method (DEIM). The method proposed applies the quadratic expansion to provide a first approximation of the non-linear operator, and DEIM is then used as a corrector to improve its representation. In addition to the treatment of the non-linear operator the POD model is stabilized using a Petrov-Galerkin method. This adds artificial dissipation to the solution of the reduced order model which is necessary to avoid spurious oscillations and unstable solutions.

A demonstration of the capabilities of this new approach is provided by simulating a flow past a cylinder and gyre problems. Comparisons are made with other treatments of non-linear operators, and these show the new method to provide significant improvements in the solution's accuracy.

Key words: Nonlinear Model Reduction,Empirical Interpolation Method, Petrov-Galerkin,Proper

*Corresponding author

Email address: `inavon@fsu.edu` (I.M. Navon)

Orthogonal Decomposition,Navier-Stokes

2. Introduction

Reduced order models (ROMs) have become important to many fields of physics as they offer the potential to simulate dynamical systems with substantially increased computation efficiency in comparison to traditional techniques. Among the model reduction techniques, the proper orthogonal decomposition (POD) method has proven to be an efficient means of deriving the reduced basis for high-dimensional nonlinear flow systems. The POD method and variants of it have been successfully applied to a number of research fields. In signal analysis and pattern recognition it is known as Karhunen-Love method[1], in statistics it is referred to as principal component analysis (PCA)[2], and in geophysical fluid dynamics and meteorology it is termed empirical orthogonal functions (EOF) [3, 4]. The POD method has since been applied to ocean models in Cao et al. [5], Vermeulen and Heemink [6] and also shallow water equations, this includes the work of Daescu and Navon [7], Chen et al. [8, 9], Altaf et al. [10], Du et al[11], as well as Fang et al. [12].

In this paper we develop a reduced order model for the reduction in the dimension of a Navier-Stokes equations using the POD approach. The equations are first discretised via a finite element Bubnov Galerkin discretisation of the Fluidity model[13] and the POD model is generated through the method of snapshots. In this approach, solutions of the full model are recorded (as a sequence of snapshots), and from this data appropriate basis functions are formed that optimally represent the problem. This method itself is quite standard and has been applied successfully throughout the literature. However, due to the high nonlinearities of the 3-D Bubnov-Galerkin Navier Stokes equation, the computational complexity of the reduced model still depends on dimension of the full Navier-Stokes discretisation [14]. To mitigate this problem, one approach is to apply the discrete empirical interpolation method (DEIM) to address the reduction of the nonlinear components and reduce the computational complexity by implementing it with the POD/DEIM method. DEIM is a discrete variant of the empirical interpolation method (EIM)[15] proposed by Barrault et al. for constructing approximation of a non-affine parameterized function, which was proposed in the context of reduced-basis model order reduction discretization of nonlinear partial differential equations. DEIM methods have been demonstrated to be able to obtain factors of 10-100 speed up in CPU time over the original non-reduced model. The economy in CPU time is proportional to the dimension of the reduced order model (see for instance Stefanescu and Navon, 2013[16]) and therefore to the number of DEIM points. The application was suggested and analysed by Chaturantabut and Sorensen[17, 18, 19] for application to POD in the framework of Discrete Empirical Interpolation Method (DEIM). Other important contributions to the Empirical Interpolation Method (EIM) include that by Barrault et al.[15] and the group of Prof Anthony Patera at MIT related to another model reduction approach namely the reduced basis approach [20, 21, 22, 23].

Regarding the use of hyper-reduced order models i.e. DEIM like approaches, they presented a strategy for choosing the optimal set of sampling points at the discrete level. The algorithm consists of selecting the sampling components that minimize the

distance between the recovered reduced basis coefficients and the optimal coefficients (which are obtained by projecting the snapshots onto the reduced order subspace). The main advantage of their algorithm is that only values at the nodes of the finite element mesh are required for the gappy reconstruction, but these sampling components can be guaranteed to be optimal. This results in a strategy very convenient for the reconstruction of non-smooth functions, like the right-hand-side of the system of equations arising from the reduced order strategy for the incompressible Navier-Stokes equations with the formulation used herein.

An alternative treatment of the non-linear terms of PDEs is through the quadratic expansion method [11]. This method is suitable for the treatment of the discretised quadratic non-linear operators as the method represents them through expansions of precomputed matrices. Critically, as these matrices are precomputed they can easily be transformed into reduced equation sets, however the method's drawback is that its accuracy will decay with the less quadratic nature of the operator.

Both the novel quadratic expansion method and novel DEIM have been developed in order to maintain the ROM's efficiency. In this article a new method is proposed which is a new hybrid of both schemes that we call residual DEIM. It is based on initially applying the quadratic expansion method to the non-linear terms and then applying the DEIM approach to resolve the residual between it and the full model. That is, the DEIM is used to absorb the remaining errors left over from the quadratic expansion approach. This approach means that the method can still exactly represent discrete quadratic non-linearities - unlike DEIM - but can also be used for highly non-linear discrete systems - unlike the quadratic expansion approach. In addition to this a non-linear Petrov-Galerkin discretization [24, 12] is used to form the ROM and stabilize the reduced system of equations, which would otherwise become unstable especially for moderate/high Reynolds number flows. This introduces additional non-linearities and thus the residual DEIM method is well suited to dealing with these potentially highly non-linear discrete systems of equations, see, for example, Baiges[25] for similar approaches. The paper demonstrates the superior accuracy of residual DEIM to the quadratic expansion method.

The structure of the paper is as follows. Section 3 presents the governing equations, followed by the description of the finite element Bubnov-Galerkin discretisation of the Navier Stokes equations. Section 4 presents the derivation of the POD model reduction and re-formulation of the Navier Stokes equations using the method of snapshots. The section concludes with the stabilization of the POD model reduction by the introduction of an adequately chosen dissipation term. Section 5 focuses on the non-linear operator treatment of the Navier-Stokes equations and describes the methods of DEIM and quadratic expansion. This section then presents the mixed residual DEIM formulation. This is based on a DEIM representation of a residual term that is left over from first applying a quadratic representation of the non-linear operator. Section 6 illustrates the methodology derived via two numerical examples. This is based on two test problems where the flow past a cylinder and flow within a gyre are resolved. Finally in section 7 conclusions are presented and the novelty of the present manuscript is duly summarized and illuminated.

3. Governing Equations

This article considers the three dimensional non-hydrostatic Navier-Stokes equations describing the conservation of mass and momentum of a fluid,

$$\nabla \cdot \mathbf{u} = 0, \tag{1}$$

$$\frac{\partial \mathbf{u}}{\partial t} + \mathbf{u} \cdot \nabla \mathbf{u} + f\mathbf{k} \times \mathbf{u} = -\nabla p + \nabla \cdot \tau. \tag{2}$$

In these equations the terms $\mathbf{u} \equiv (u_x, u_y, u_z)^T$ denote the velocity vector, p the perturbation pressure ($p := p/\rho_0$, ρ_0 is the constant reference density) and f the Coriolis inertial force. The stress tensor τ included in the diffusion term represents the viscous forces, and this is defined in terms of a deformation rate tensor $\mathbf{S}$ which is given as,

$$\tau_{ij} = 2\mu_{ij}S_{ij}, \quad S_{ij} = \frac{1}{2}\left(\frac{\partial u_i}{\partial x_j} + \frac{\partial u_j}{\partial x_i}\right) - \frac{1}{3}\sum_{k=1}^{3}\frac{\partial u_k}{\partial x_k}, \quad i, j = \{x, y, z\}. \tag{3}$$

In this expression μ denotes the kinematic viscosity and it is assumed that there is no summation over repeated indices. The horizontal (μ_{xx}, μ_{yy}) and vertical (μ_{zz}) kinematic viscosities are assumed to take constant values and define the off diagonal components of τ in equation 3 by $\mu_{ij} = (\mu_{ii}\mu_{jj})^{1/2}$. For barotropic flow, the pressure p consists of hydrostatic $p_h(z)$ and non-hydrostatic $p_{nh}(x, y, z, t)$ components. The hydrostatic component of pressure balances the constant buoyancy force exactly, and so both terms are neglected at this stage. The momentum equation can be expressed more fully as,

$$A_t\frac{\partial \mathbf{u}}{\partial t} + A_x(\mathbf{u})\frac{\partial \mathbf{u}}{\partial x} + A_y(\mathbf{u})\frac{\partial \mathbf{u}}{\partial y} + A_z(\mathbf{u})\frac{\partial \mathbf{u}}{\partial z} + f\mathbf{k} \times \mathbf{u} + \nabla p - \nabla \cdot \tau = 0, \tag{4}$$

where the time term A_t and streaming operators A_x, A_y and A_z denote diagonal matrices that are given by,

$$A_t = \begin{pmatrix} 1 & 0 & 0 \\ 0 & 1 & 0 \\ 0 & 0 & 1 \end{pmatrix}, \tag{5}$$

and

$$A_x = \begin{pmatrix} u_x & 0 & 0 \\ 0 & u_x & 0 \\ 0 & 0 & u_x \end{pmatrix}, \quad A_y = \begin{pmatrix} u_y & 0 & 0 \\ 0 & u_y & 0 \\ 0 & 0 & u_y \end{pmatrix}, \quad A_z = \begin{pmatrix} u_z & 0 & 0 \\ 0 & u_z & 0 \\ 0 & 0 & u_z \end{pmatrix}, \tag{6}$$

respectively.

In this article a finite element Bubnov-Galerkin discretisation of the Navier Stokes equations [13] is employed. In this formulation the velocity components and pressure terms of the solution are represented by the expansions,

$$u_x = \sum_j^{F_u} N_j u_{xj}, \; u_y = \sum_j^{F_u} N_j u_{yj}, \; u_z = \sum_j^{F_u} N_j u_{zj}, \tag{7}$$

and

$$p = \sum_j^{F_p} M_j p_j, \tag{8}$$

respectively, where N_j and M_j denote the finite element basis functions. To solve for the coefficients $u_{.j}$ and p_j the discretised equations are formed by weighting equations 1 and 2 by M_i and N_i, respectively, and integrating over space,

$$\int_v M_i \nabla \cdot \mathbf{u} \, dv = 0, \tag{9}$$

$$\int_v N_i \frac{\partial \mathbf{u}}{\partial t} + \mathbf{u} \cdot \nabla \mathbf{u} + f\mathbf{k} \times \mathbf{u} \, dv = -\nabla p + \nabla \cdot \tau. \tag{10}$$

When the approximations 7 and 8 are inserted into these equations the following systems are formed,

$$C^t u = 0,$$

$$N \frac{\partial \mathbf{u}}{\partial t} + A(\mathbf{u})\mathbf{u} + K\mathbf{u} + Cp = s. \tag{11}$$

In these equations the matrix C denotes the pressure gradient matrix, N is the mass matrix involving the finite element basis functions N_i, $A(u)$ is the solution dependent discretised streaming operator, K is the matrix related to the rest of the linear terms of velocity, and s is the vector accounting for the forces acting upon the solution. In the momentum equation the time term is treated using the θ-method to yield,

$$N \frac{\mathbf{u}^{n+1} - \mathbf{u}^n}{\Delta t} + A(\mathbf{u}^n)\mathbf{u}^{n+\theta} + K\mathbf{u}^{n+\theta} + Cp^{n+1} = 0, \tag{12}$$

where $\theta \in [0, 1]$ and the terms $\mathbf{u}^{n+\theta}$ is given by,

$$\mathbf{u}^{n+\theta} = \theta \mathbf{u}^{n+1} + (1 - \theta)\mathbf{u}^n. \tag{13}$$

The full system of equations can now be grouped together to form the general linear system for each time step,

$$\begin{bmatrix} B & C \\ C^T & 0 \end{bmatrix} \begin{bmatrix} \mathbf{u}^{n+1} \\ p^{n+1} \end{bmatrix} = \begin{bmatrix} B' & 0 \\ 0 & 0 \end{bmatrix} \begin{bmatrix} \mathbf{u}^n \\ p^n \end{bmatrix} + \begin{bmatrix} s \\ 0 \end{bmatrix}, \tag{14}$$

where B and B' are matrices of similar form but differ through the choice of θ. In this system the matrix B is non-linear as it depends on the solution $\mathbf{u}$. On the RHS, the vector $[s, 0]^T$ contains the discretised sources and the terms within the matrix system account for the solution from the previous time step.

Alternative but identical expressions of the above system of equations can be written in order to help develop the methods derived in the following sections. One expression is derived by condensing the expression into the single system of equations given by,

$$P(y)y^{n+1} = Q(y)y^n + s, \tag{15}$$

where y^n denotes the full solution vector at time step n, i.e. the concatenation of all velocity and pressure components. Another representation of this equation is to rewrite system 15 with separated linear (L superscript) and non-linear (N superscript) terms,

$$(P^L + P^N)y^{n+1} = (Q^L + Q^N)y^n + s. \tag{16}$$

The following theory will be built upon one of these identical expressions of the discretised Navier-Stokes equations.

4. POD method for the Navier-Stokes Equations

In the following subsections the POD method is described together with its application to the modelling of the Navier-Stokes equation and its stabilisation. In the theory that follows in this and the next section the notation becomes quite involved and so table 1 has been included in order to make clear the variable definition.

Variable	Definition
S	Total number of arbitrary snapshot set.
S_u	Total number of snapshot for velocity components.
S_p	Total number of snapshot for pressure components.
F	Total number of nodes on arbitrary finite element discretisation.
F_u	Total number of nodes on finite element discretisation of the velocity.
F_p	Total number of nodes on finite element discretisation of the pressure.
P	Total function in an arbitrary POD basis set.
P_u	Total number of functions in the velocity POD basis set.
P_p	Total number of functions in the pressure POD basis set.
Φ	General POD basis functions.
Φ_p	Standard POD basis functions.
Φ_d	DEIM POD basis functions.

Table 1: The table lists the variables and their definition used in this article.

4.1. The POD Model

In the POD formulation a new set of basis functions are constructed from a collection of snapshots that are taken at a number of time instances of the full model solution. That is, the model described in equation 14 is solved and snapshots of the solution are taken as it evolves through time. In the formulation presented here snapshots of each component of the velocity vector (u_x, u_y, u_z) and pressure p are recorded individually. Each snapshot is a vector of size F_u or F_p (depending on whether it is of a velocity component of pressure term) and holds the values of the respective solution component at the nodes of the finite element mesh. For each direction or pressure component, these snapshots are collated together over all time instances to form four separate matrices $\mathcal{U}^x, \mathcal{U}^y, \mathcal{U}^z$ and $\mathcal{U}^p$ (where the superscripts denote direction or pressure). From here on each snapshot matrix will be treated separately but in an identical manner, and so the superscripts are omitted and the details are given for a general snapshot matrix $\mathcal{U}$.

The dimensions of $\mathcal{U}$ is $F \times S$, where F denotes the general number of nodes on the finite element mesh and S the total number of snapshots (this will be of value S_u and S_p for the velocity and pressure, respectively). Once the full set of snapshots have been collated, it is then custom to remove from each snapshot the mean value of all snapshots. That is, a modified snapshot matrix $\overline{\mathcal{U}}$ is generated by,

$$\overline{\mathcal{U}}_{k,i} = \mathcal{U}_{k,i} - \overline{\Phi}_i, \quad i \in \{1, 2, \ldots, S\}, \tag{17}$$

where the vector $\overline{\Phi}$ (of size F) holds the average value of all snapshot on each node i:

$$\overline{\Phi}_i = \frac{1}{N_k} \sum_{j=1}^{N_k} \mathcal{U}_{j,i}, \quad i \in \{1, 2, \ldots, F\}. \tag{18}$$

A reduced-order basis set of functions $\{\Phi_u\}$ are now obtained by means of the Proper Orthogonal Decomposition method. This involves performing a Singular Value Decomposition (SVD) of the snapshot matrix $\overline{\mathcal{U}}$ given by the form,

$$\overline{\mathcal{U}} = U \Sigma V^T, \tag{19}$$

The terms U and V are unitary matrices of dimension $F \times F$ and $S \times S$, respectively, and Σ is a diagonal matrix of size $F \times S$. The non zero values of Σ are the singular values of $\overline{\mathcal{U}}$, and these are assumed to be listed in order of their magnitude. It can be shown [17] that the POD functions can be defined as the column vectors of the matrix U,

$$\Phi_j = U_{:,j}, \qquad \text{for } j \in \{1, 2 \ldots S\}, \tag{20}$$

and the optimal basis set of size P are the functions corresponding to the largest P singular values (i.e. the first P columns of U). These functions are optimal in the sense that no other rank P set of basis functions can be closer to the snapshot matrix $\overline{\mathcal{U}}$ in the Frobenius norm. That is, if one used only the first P singular values in equation 20 (and so the first P vectors in U), the resulting matrix is the closest possible (in the relevant norm) to the matrix $\overline{\mathcal{U}}$. Another relevant property is that due to U being unitary, the POD vectors are orthonormal.

To efficiently construct the POD vectors defined by U one of two approaches may be taken. Depending on the dimensions of $\overline{\mathcal{U}}$ a reduced symmetric linear system can be formed by the pre or post multiplication of $\overline{\mathcal{U}}$ by its transpose. If the number of finite element nodes are smaller than the number of snapshots ($F << S$), then post multiplying by $\overline{\mathcal{U}}^T$ results in an $F \times F$ system with the property,

$$\overline{\mathcal{U}}\overline{\mathcal{U}}^T = U \Lambda^2 U^T. \tag{21}$$

This enables one to perform an eigenvalue decomposition on the system 21 to obtain U directly. Alternatively, if the number of snapshots is smaller than the number finite element functions ($S << F$), the pre multiplication of $\overline{\mathcal{U}}$ by $\overline{\mathcal{U}}^T$ results in,

$$\overline{\mathcal{U}}^T \overline{\mathcal{U}} = V^T \Lambda^2 V \tag{22}$$

In this case one can perform the eigenvalue decomposition of system 22 to obtain the matrix V and singular values Λ. Once these are available the vectors of U can be formed by substituting into system 19.

As mentioned previously, only a small number of P POD functions are used in the reduced order model. Although these POD functions provide an optimal representation of the snapshot matrix, some information is inevitably lost. This loss of information

can be quantified by the following ratio, which is usually termed energy, of the squared singular values,

$$I = \frac{\sum_{i=1}^{P} \Lambda_{i,i}^2}{\sum_{i=1}^{S} \Lambda_{i,i}^2}. \tag{23}$$

The value of I will tend to 1 as P is increased to the value S, and so this value can be used to provided an appropriate truncation point of the POD expansion set. Having set the size P, the P POD functions can now be used to form a basis that represents the snapshot data set. That is, a vector u of size F can be represented by the expansion,

$$u = \overline{\Phi} + \sum_{j}^{P} \alpha_j \Phi_j, \tag{24}$$

where α_j denote the expansion coefficients.

4.2. Forming the POD formulation of the Navier Stokes Equations

To form the reduced order system of the Navier Stokes equations, the velocity and pressure components are expanded over their respective POD basis functions. Their finite element solution variables (equation 14) are re-written in the form of equation 24 to give,

$$u_x^n = \overline{\Phi}^x + \sum_{j}^{P_u} \alpha_j^{x,n} \Phi_j^x, \quad u_y^n = \overline{\Phi}^y + \sum_{j}^{P_u} \alpha_j^{y,n} \Phi_j^y, \quad u_z^n = \overline{\Phi}^z + \sum_{j}^{P_u} \alpha_j^{z,n} \Phi_j^z, \tag{25}$$

for the velocities and,

$$p^n = \overline{\Phi}^p + \sum_{j}^{P_p} \alpha_j^{p,n} \Phi_j^p, \tag{26}$$

for the pressure. The POD expansion sizes of the velocity and pressure terms are denoted by P_u and P_p respectively, and the α terms denote the expansion coefficients. These expansions can be represented in the following matrix vector form,

$$u^n = \overline{\Phi}^x + \Phi^x \alpha^{x,n}, \;\; v^n = \overline{\Phi}^y + \Phi^y \alpha^{y,n}, \;\; w^n = \overline{\Phi}^z + \Phi^z \alpha^{z,n}, \;\; p^n = \overline{\Phi}^p + \Phi^p \alpha^{p,n}, \tag{27}$$

where Φ^x, Φ^y and Φ^z denote matrices of size $F_u \times P_u$, Φ^p is a matrix of size $F_p \times P_p$, $\overline{\Phi}^x$, $\overline{\Phi}^y$ and $\overline{\Phi}^z$ are vectors of size F_u and $\overline{\Phi}^p$ is a vector is a vector of size F_p.

If the solution variables are also represented by a single vector, as in equation 15, then the reduced order representation can also read as,

$$y^n = \begin{bmatrix} u_x \\ u_y \\ u_z \\ p \end{bmatrix}^n = \overline{\Phi}^y + \Phi^y \alpha^{y,n} = \begin{bmatrix} \overline{\Phi}^x \\ \overline{\Phi}^y \\ \overline{\Phi}^z \\ \overline{\Phi}^p \end{bmatrix} + \begin{bmatrix} \Phi^x & 0 & 0 & 0 \\ 0 & \Phi^y & 0 & 0 \\ 0 & 0 & \Phi^z & 0 \\ 0 & 0 & 0 & \Phi^p \end{bmatrix} \begin{bmatrix} \alpha^{x,n} \\ \alpha^{y,n} \\ \alpha^{z,n} \\ \alpha^{p,n} \end{bmatrix}. \tag{28}$$

This is an identical expression to those of equation 27 since the terms $\overline{\Phi}^y$ and Φ^y are formed from the combination of all the POD matrices and vectors. The coefficients

in the discretised system 14 (or 15) are then replaced by their POD representation of equation 27 (or 28), and the resulting system is pre-multiplied by the transpose of the POD matrices in order to form the reduced system. For now we work on the equation in the form of 14 and the reduced system reads as,

$$\begin{bmatrix} B^{POD} & C^{POD} \\ (C^{POD})^T & 0 \end{bmatrix} \begin{bmatrix} \alpha^{u,n+1} \\ \alpha^{p,n+1} \end{bmatrix} = \begin{bmatrix} B'^{POD} & 0 \\ 0 & 0 \end{bmatrix} \begin{bmatrix} \alpha^{u,n} \\ \alpha^{p,t} \end{bmatrix} - \begin{bmatrix} \overline{s}^u \\ \overline{s}^p \end{bmatrix} + \begin{bmatrix} s^{POD} \\ 0 \end{bmatrix}. \tag{29}$$

It can be seen that the system retains the same structure of the original full system in equation 14. The reduced matrix B^{POD} is of size $3P_u \times 3P_u$ and can be written as $B^{POD} = (\Phi^u)^T B \Phi^u$ (with a similar expression of B'^{POD}) where,

$$\Phi^u = \begin{bmatrix} \Phi^x & 0 & 0 \\ 0 & \Phi^y & 0 \\ 0 & 0 & \Phi^z \end{bmatrix}. \tag{30}$$

Similarly the matrix C^{POD} is a reduced system of size $3P_u \times P_p$ and this is given by $C^{POD} = (\Phi^u)^T C \Phi^p$. The reduced source terms is a vector of size P_u and is formulated as $s^{POD} = (\Phi^u)^T s$. The additional source terms in equation 29 result from contribution of the average snapshot vectors, and these are given by,

$$\begin{bmatrix} \overline{s}^u \\ \overline{s}^p \end{bmatrix} = \begin{bmatrix} (\Phi^u)^T B \overline{\Phi}^u + (\Phi^u)^T C \overline{\Phi}^p \\ (\Phi^p)^T C \overline{\Phi}^u \end{bmatrix}. \tag{31}$$

4.3. Stabilisation of the POD Model

The POD model described in equation 29 will often require an additional modification through a stabilisation term to ensure it remains stable and free from unphysical oscillations. The full details of the stabilisation technique is described in full in [24] , and so only the main concepts are reviewed here. Stabilisation is added to the model though an additional diffusion operator. It is included into the LHS matrix of equation 29 by adding to it the block diagonal diffusion matrix,

$$\mathbf{D} = \begin{pmatrix} \mathbf{D}_x & 0 & 0 & 0 \\ 0 & \mathbf{D}_y & 0 & 0 \\ 0 & 0 & \mathbf{D}_z & 0 \\ 0 & 0 & 0 & \mathbf{D}_p \end{pmatrix}. \tag{32}$$

This matrix is size $(3P_u + P_p) \times (3P_u + P_p)$ and is composed of the three sub-matrices,

$$\mathbf{D}_{x_{ij}} = \int_V \nabla \Phi_i^x \mu_x \nabla \Phi_j^x \, dV, \tag{33}$$

$$\mathbf{D}_{y_{ij}} = \int_V \nabla \Phi_i^y \mu_y \nabla \Phi_j^y \, dV, \tag{34}$$

$$\mathbf{D}_{z_{ij}} = \int_V \nabla \Phi_i^z \mu_z \nabla \Phi_j^z \, dV, \tag{35}$$

$$\tag{36}$$

that are of size $P_u \times P_u$ and the matrix,

$$\mathbf{D}_{p_{ij}} = \int_V \nabla\Phi_i^p \mu_p \nabla\Phi_j^p \, dV, \tag{37}$$

which is of size $P_p \times P_p$. Each matrix places diffusion in their respective velocity or pressure terms, and the amount of diffusion is governed by the coefficients μ. The calculation of the diffusion coefficients are detailed in [24] and so are omitted here. However it is important to stress that its inclusion introduces strong non-quadratic non-linearities to the formulation that must be resolved by the following reduced order schemes. In this work it was not necessary to stabilise the pressure and so the diffusion coefficient relating to it has been set to zero.

5. Efficient treatments of the Non-linear operators

In the following sections a review of the current approaches to resolving the non-linear operators are presented. This is then followed by the details of the proposed residual DEIM method.

5.1. DEIM treatment of the Non-Linear Operator

This section presents the application of DEIM which will be used in the following sections to resolve the non-linear terms of the Navier-Stokes equations within an efficient reduced order model. For now the method is described in the general sense for an arbitrary differential equation that is expressed in terms of its linear (L) and non-linear (N) components. When discretised through a finite element representation the following model is formed,

$$\frac{dy}{dt}(t) = Ly(t) + N(y(t)), \;\; A \in \mathbb{R}^{F\times F}. \tag{38}$$

In this equation the new solution variables $y(t) = [y_1(t), y_2(t), .., y_F(t)] \in \mathbb{R}^F$ define the solution's values over the F nodes of the finite element mesh. As the term N is a non-linear function it requires y(t) to be evaluated component wise at each time instance t, i.e. $N = [N(y_1(t)), .., N(y_F(t))]$. It is this re-evaluation that makes the reduced order modelling inefficient if the standard POD approach (as described in the previous section) is applied. This is because if the nonlinear term is represented through a POD model, i.e. it is pre and post multiplied by Φ_p^T and Φ_p respectively (the subscript p denotes standard POD functions), the resulting reduced space formulation will read as,

$$\tilde{N}(\tilde{y}) = \underbrace{\Phi_p^T}_{P\times F} \underbrace{N(\Phi_p \tilde{y}(t))}_{F\times 1} = \underbrace{\Phi_p^T}_{P\times F} \underbrace{f(t)}_{F\times 1}. \tag{39}$$

This expression shows that even in the reduced space, the model requires an operation with complexity of order F at each time step. The model is therefore no longer efficient to compute, i.e. it is the same order of the non-reduced model, and so an alternative approach must be applied.

The DEIM approach is one such method used to treat the non linear terms of PDEs within a reduced order framework. The approach is to use a separate POD model to construct a basis of the space spanned by the non-linear components of the equation. That is, a snapshot matrix $\mathcal{U}_d$ of the non-linear terms is constructed by,

$$\mathcal{U}_d = \{N(y_1), N(y_2), \ldots, N(y_n)\}, \tag{40}$$

from which a POD model is built using the approach described in the previous section. Using Φ_d to denote this POD basis set, which is analogous to that in equation 20, the term $f(t)$ in equation 39 can be represented by,

$$f(t) = \Phi_d c(t). \tag{41}$$

The dimension of Φ_d is of $F \times D$, where D denotes the size of the reduced representation of the nonlinear terms ($D << F$) and $c(t)$ is a coefficient vector of size D that has yet to be determined. If one now inserts 41 into 39 the following results,

$$\tilde{N}(\tilde{y}) = \underbrace{\Phi_p^T \Phi_d}_{P \times D} \underbrace{c(t)}_{D \times 1}, \tag{42}$$

for which the matrix in this expression is time independent. The matrix can therefore be precomputed, which in turn means that once $c(t)$ is known, the non linear expression can be computed with order of complexity D.

The vector $c(t)$ is constructed by solving a reduced form of the over determined system 41, and this is given by,

$$\underbrace{\Phi_{d\rho}}_{\mathbb{R}^{D \times D}} \underbrace{c(t)}_{\mathbb{R}^D} = \underbrace{f_\rho(t)}_{\mathbb{R}^D}, \tag{43}$$

where the $c(t)$ vector remains the same as that in the original system. The new system in equation 43 is of size $D \times D$, and this is formed by extracting D rows from the original $F \times D$ system. The selection of which rows (or interpolation points) to use is discussed in [17, 26], but once determined the selected row indices are indicated by the indexing vector $\hat{\rho}$, which is of size D (i.e. if the k^{th} selected point corresponds to row i then $\hat{\rho}_k = i$). Using this vector the elements of the system 43 are given as,

$$\{\Phi_{d\rho}\}_{ij} = \{\Phi_d\}_{\hat{\rho}_i \hat{\rho}_j}, \textit{and} \quad f_\rho(t)_i = f(t)_{\hat{\rho}_i}, \tag{44}$$

respectively. Provided that the matrix is invertible, the system 43 can be solved to obtain $c(t)$,

$$c(t) = \Phi_{d\rho}^{-1} f_\rho(t). \tag{45}$$

One can now generate the matrix $P = [e_{\rho_1}, .., e_{\rho_m}] \in \mathbb{R}^{F \times D}$, which is formed from the vectors e_i which have the value 1 in their component ρ_i and zero else where, that is $e_{\rho_i} = [0, 0, .., \underbrace{1}_{\rho_i}, .., 0, 0]^T \in \mathbb{R}^F$. This matrix can be used to represent the reduced components in equation 45 through their original matrices and vectors by,

$$\Phi_{d\rho} = P^T \Phi_d, \tag{46}$$

and

$$f_\rho(t) = P^T f(t), \tag{47}$$

respectively. Expression 45, 46 and 47 can now be combined and used within 41 to give the following formulation,

$$f(t) = \Phi_d (P^T \Phi_d)^{-1} P^T f(t). \tag{48}$$

The final form of the reduced model of the non-linear component can now be formed by inspecting equation 39 and noting that,

$$f_\rho(t) = P^T f(t) = P^T F(\Phi_p \tilde{y}(t)) = F(P^T \Phi_p \tilde{y}(t)). \tag{49}$$

Replacing this expression inside 49 gives,

$$f(t) = \Phi_d (P^T \Phi_d)^{-1} F(P^T \Phi_p \tilde{y}(t)), \tag{50}$$

which is then substituted within 39 to give the final form of the non-linear reduced order model,

$$\tilde{N}(\tilde{y}) \approx \underbrace{\Phi_p^T \Phi_d (P^T \Phi_d)^{-1}}_{\text{precomputed } P\times D} \underbrace{F(P^T \Phi_p \tilde{y}(t))}_{D\times 1}. \tag{51}$$

As indicated, the computationally expensive matrix can be precomputed due to its time independence. Therefore, at each time instance of the reduced order model, only a matrix vector multiplication involving a system of the size $N_p \times N_d$ is required.

5.2. Quadratic expansion of the Non-Linear Operator

An alternative approach for efficiently treating the non-linear terms within a reduced order model is through the quadratic expansion method proposed in [11]. The approach is reviewed here by considering the matrix operator B in equation 14, for which the non-linear components arise from the streaming operator in the Navier Stokes equation. The matrix is re-written by the following summation involving the $P_u + 1$ sub-matrices,

$$B = \overline{B} + \sum_{i=1}^{P_u} \hat{B}_i. \tag{52}$$

In this expression the matrix $\overline{B}$ is of size $3F_u \times 3F_u$, and this is dependent on the average velocity components $\overline{u}$, i.e. $\overline{B} = B(\overline{u})$. The matrices $\hat{B}_i$ in the summation are also of size $3F_u \times 3F_u$ and these are decomposed further into the following form,

$$\hat{B}_i = \begin{bmatrix} \alpha_i^1 \hat{B}_i^x & 0 & 0 \\ 0 & \alpha_i^2 \hat{B}_i^y & 0 \\ 0 & 0 & \alpha_i^3 \hat{B}_i^z \end{bmatrix}. \tag{53}$$

Here the sub-matrices $\hat{B}_i^j$ are of size $F_u \times F_u$ and these are dependent on the i^{th} POD function that is associated with direction component j. In this expression the expansion multiplies the matrices by their respective POD coefficients α_i^j, however the sub-matrices themselves are fixed and so can be precomputed. The precomputing can be

accomplished by considering a perturbation to the average vector $\overline{u}$. The perturbations are defined in the POD space, and so three vectors of size P_u are created that relate to all POD functions for each of the three velocity components. Their values are all set to zero except for a small perturbation ϵ in one element of a vector. For example, in the vector relating to the direction x, the i^{th} perturbation is given by,

$$\epsilon_i^x = \{0, \ldots, 0, \underbrace{\epsilon}_{i}, 0 \ldots, 0\},\ \epsilon_i^y = \{0, \ldots, 0, \ldots, 0\},\ \epsilon_i^z = \{0, \ldots, 0, \ldots, 0\}. \tag{54}$$

These perturbed POD coefficients provide a the perturbed velocity solution given as,

$$\tilde{u} = \begin{bmatrix} u^x \\ u^y \\ u^z \end{bmatrix} = \overline{u} + \begin{bmatrix} \epsilon\Phi^x \\ 0 \\ 0 \end{bmatrix}, \tag{55}$$

which can be used in expression 52 to give the expression of $\hat{B}_i^j$,

$$\hat{B}_i^j = \frac{1}{\epsilon}(B(\tilde{u}) - B(\overline{u})). \tag{56}$$

The same approach can be applied to obtain all matrices in the summation 52, and once computed they can be represented in the reduced space by their projection with the POD functions. That is,

$$\hat{B}_i^{POD} = (\Phi^u)^T \hat{B}_i \Phi^u, \tag{57}$$

which are in turn used to define the reduced B matrix,

$$B^{POD} = \overline{B}^{POD} + \sum_i^{P_u} \hat{B}_i^{POD}, \tag{58}$$

where $\overline{B}^{POD} = (\Phi^u)^T \overline{B} \Phi^u$ is the projection of $\overline{B}$ onto the reduced space.

5.3. The Residual DEIM Method

A mixed DEIM-quadratic expansion formulation of the nonlinear reduced order operator is now derived. It is based on a DEIM representation of a residual term that is left over from first applying a quadratic representation of the non-linear operator. The method is derived from equation 16 which represents the full model discretised into its linear and non-liner components. The system is now rewritten as,

$$(P^L + P_f^N + P_q^N - P_q^N)y^{n+1} = (Q^L + Q_f^N + Q_q^N - Q_q^N)y^n + s, \tag{59}$$

where the subscripts f and q denote the full and quadratic operators, respectively. This is then re-arranged into the form of

$$(P^L + P_q^N)y^{n+1} = (Q^L + Q_q^N)y^n + s + \{(-Q_f^N + Q_q^N)y^n + (-P_f^N + P_q^N)y^{n+1}\}. \tag{60}$$

The system on the left hand side now only contains a linear and a nonlinear component that is represented by the quadratic expansion. This and the first two terms on the

RHS (which also contain only quadratic representations of the non-linear terms) are therefore re-cast into an efficient reduced order model using the method described in sections 4.2 and 5.2. These reduced systems (denoted with a $\tilde{.}$) are given by,

$$\tilde{P}^L = \Phi_p^T P^L \Phi_p, \quad \tilde{Q}^L = \Phi_p^T Q^L \Phi_p \quad \text{and} \quad \tilde{b} = \Phi_p^T b \tag{61}$$

for the linear terms and

$$\tilde{P}^N = \Phi_p^T P^N \Phi_p \quad \text{and} \quad \tilde{Q}^L = \Phi_p^T Q^L \Phi_p, \tag{62}$$

for the non linear quadratic terms (note that the terms P^N and Q^N have representations as given in equation 52).

The remaining term on the RHS of 60 (closed within the brackets) is the residual that is formed from applying the quadratic approximation of the non-linear operator. These operators are also non-linear and so it is these that are represented by the DEIM method. That is, the non-linear operator relating to equation 38 in the DEIM formulation is expressed as,

$$N(y(t)) = (-Q_f^N + Q_q^N)y^n + (-P_f^N + P_q^N)y^n, \tag{63}$$

which in turn has the reduced order formulation,

$$\tilde{N}(\tilde{y}) = \Phi_p^T \Phi_d (P^T \Phi_d)^{-1} P^T F(\Phi_p \tilde{y}(t)). \tag{64}$$

Together the new reduced order model, which has been named the residual DEIM model, reads as,

$$(\tilde{P}^L + \tilde{P}^N)\tilde{y}^{n+1} = (\tilde{Q}^L + \tilde{Q}^L)\tilde{y}^n + \tilde{b} + \tilde{N}(\tilde{y}) \tag{65}$$

6. Numerical Examples

A demonstration in the use of the reduced order modelling scheme is presented in this section. This is based on two test problems where the flow past a cylinder and flow within a gyre are resolved. Both problems were initially solved in order to obtain a full solution, and this was through the use of the fluidity model that is formulated within a finite element framework [13]. This applied a $P_{1DG}P2$ finite element formulation using unstructured triangular meshes, and in both test cases a sufficiently resolved mesh was used to ensure an accurate solution was obtained. From these full model simulations the snapshots of both the solution variables and the non-linear terms were taken. Using this snapshot data the reduced order models were then formed and used to re-solve the problems.

In this demonstration a comparison between the quadratic treatment of the non-linear terms and the residual DEIM approach has been made. In addition to comparing solution profiles the analysis compares the solution errors as well as correlation coefficients. The measured error is given by the root mean square error (RMSE) which is calculated for each time step n by,

$$RMSE^n = \sqrt{\frac{\sum_{i=1}^{F}(\psi_i^n - \psi_{o,i}^n)^2}{F}}. \tag{66}$$

In this expression ψ_i^n and $\psi_{o,i}^n$ denote the POD (mapped onto the full mesh) and full model solution at the node i, respectively, and F represents number of nodes on the full mesh. The correlation coefficient is computed for each time step, and is defined for given expected values μ_{ψ^n} and $\mu_{\psi_o^n}$ and standard deviations σ_{ψ^n} and $\sigma_{\psi_o^n}$,

$$corr(\psi^n, \psi_o^n)^n = \frac{cov(\psi^n, \psi_o^n)}{\sigma_{\psi^n}\sigma_{\psi_o^n}} = \frac{E(\psi^n - \sigma_{\psi^n})(\psi_o^n - \sigma_{\psi_o^n})}{\sigma_{\psi^n}\sigma_{\psi_o^n}}. \tag{67}$$

6.1. Case 1: Flow past a cylinder

In the first numerical example a 2 dimensional flow past a cylinder is simulated. The problem domain is 50 units in length and 10 units in width, and it possesses a cylinder of radius 3 units positioned over the point (5,5). The dynamics of the fluid flow is driven by an in-flowing liquid with velocity 1 unit/sec, and this enters the domain through the left boundary. The fluid is allowed to flow past the cylinder and out the domain through the right boundary. No slip and zero outward flow conditions are applied to the upper and lower edges of the problem whilst Dirichlet boundary conditions are applied to the cylinder's wall. The properties of the fluid are such that the Reynolds number for this problem is calculated to be $Re = 3200$.

The problem was simulated for a period of 10 seconds, and for all models a time step size of $\Delta t = 0.01$ was used. From the full model simulation, with a mesh of 3213 nodes, 375 snapshots were obtained at equal time intervals for each of the u, v and p solution variables. Similarly, 375 snapshots of the corresponding non-linear residual profiles, as described in equation 63, were also taken. Figure 1 presents the distribution of the interpolation points when using DEIM to represent the residual terms. These points can be thought as providing an indication as to where the quadratic expansion method provides the least accurate reconstruction of the non-linear operators.

Figures 2 - 4 present the simulated flow patterns at time instances 3.52 and 10.0 seconds. They compare the full solution against reduced order model using both the quadratic expansion and the residual DEIM methods. In each of the figures the number of POD functions used in the simulation increases from 12 to 48 and then 96 functions. In the residual DEIM calculations the number of interpolation points was set to the same number of POD functions used. From these flow patterns it is shown that both the quadratic expansion and residual DEIM methods are capable of capturing the solution's main structural details. It is also shown that the residual DEIM performs very well using as few as 12 functions. In addition, the magnitude of the residual DEIM profiles appears to be in closer agreement to the full model solutions. This is highlighted in the graphs presented in figure 5 which show the solution velocities at 3 points in the domain. The results highlight how the residual DEIM method improves the quadratic expansion method by suppressing the over and under shoots that form in its solution.

The graphs in figures 6 and 7 show the two reduced order method's errors and correlation coefficients. The graphs presenting the errors show a noticeable improvement in accuracy using the residual DEIM method where by the errors are reduced by approximately 80%. The correlation graphs show the quadratic expansion's coefficient to vary about the values 0.6-0.8 where as for residual DEIM the values remain around 0.9-0.98. This again illustrates the improved accuracy gained in using this new approach.

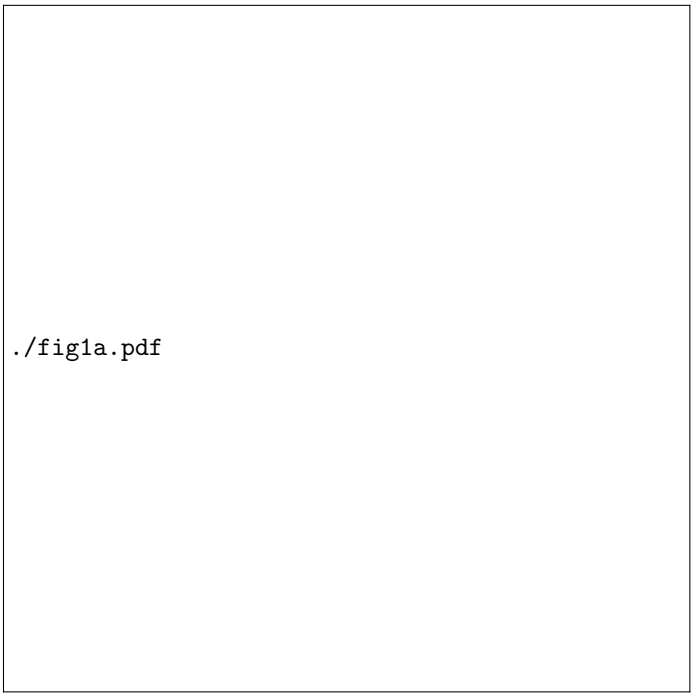

(a) 12 DEIM points for residual DEIM

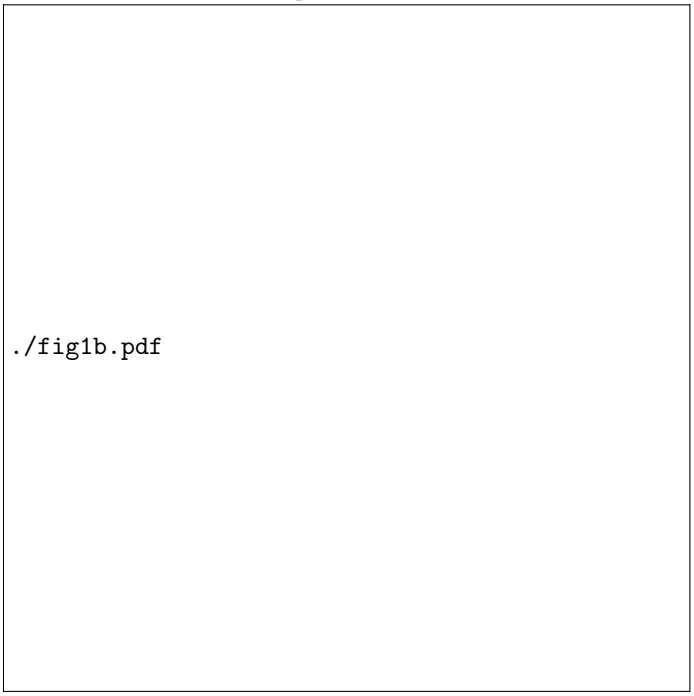

(b) 48 DEIM points for residual DEIM

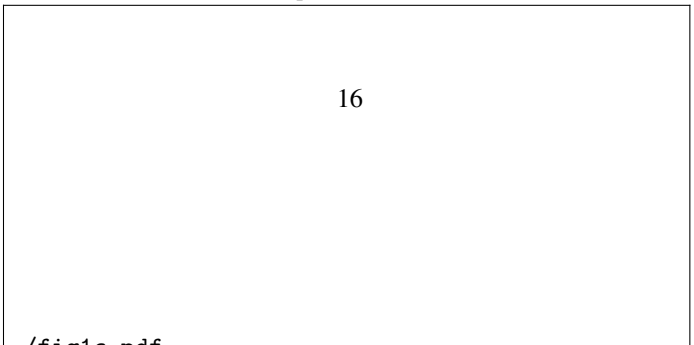

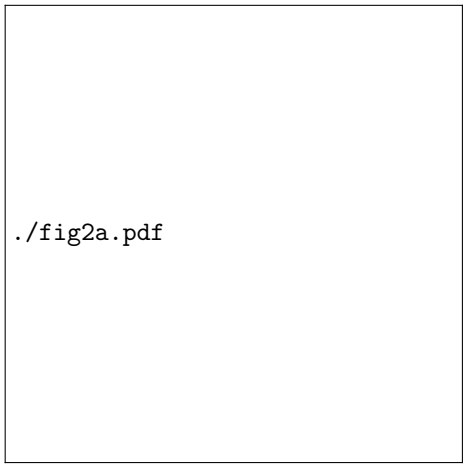

(a) full model, $t = 3.52$

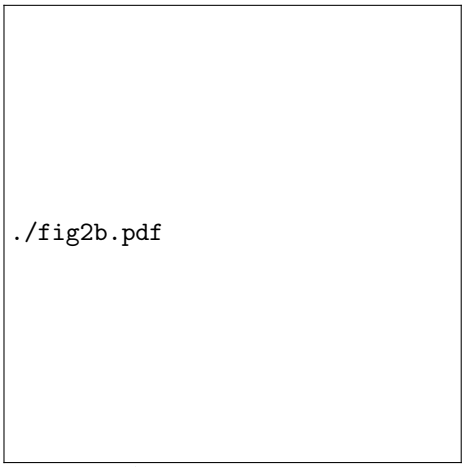

(b) full model, $t = 10.0$

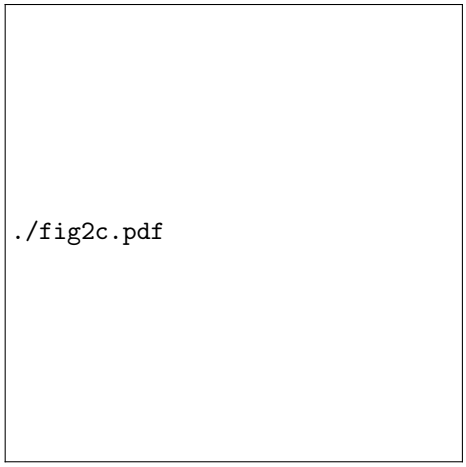

(c) Quadratic expansion, $t = 3.52$

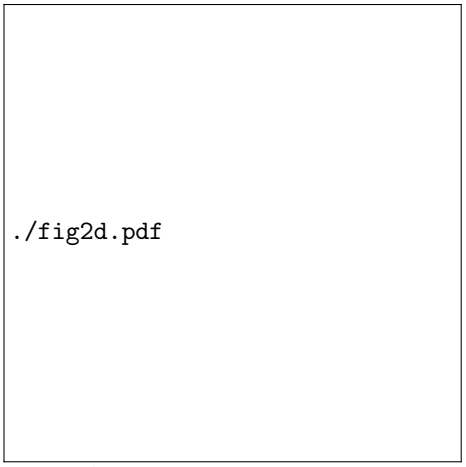

(d) Quadratic expansion, $t = 10.0$

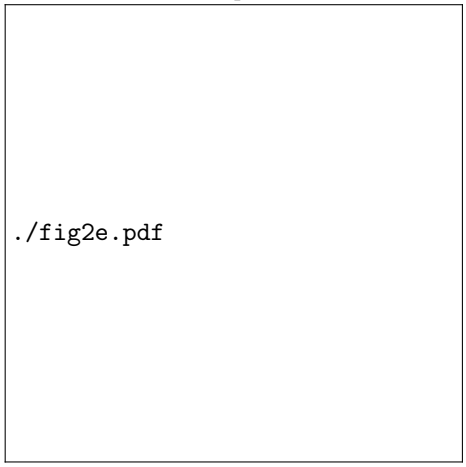

(e) Residual DEIM, $t = 3.52$

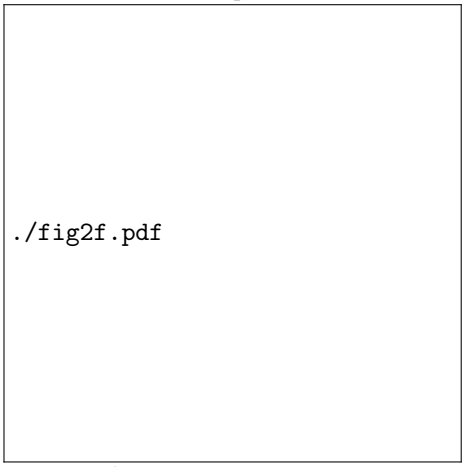

(f) Residual DEIM, $t = 10.0$

Figure 2: These show the solutions of the flow past a cylinder problem at time instances 3.52 and 10.0 seconds. The solutions compare the predictions from the quadratic expansion and residual DEIM models using 12 POD basis functions.

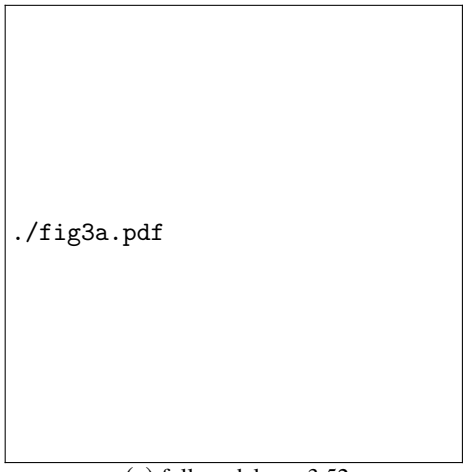

(a) full model, $t = 3.52$

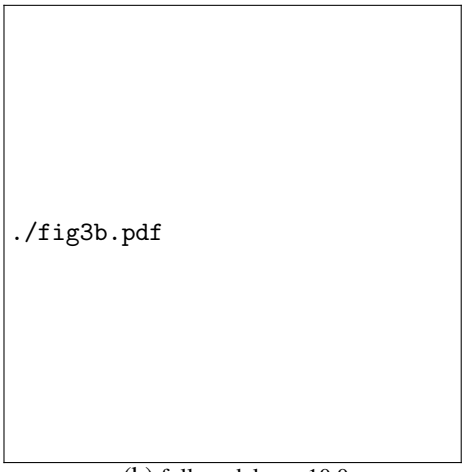

(b) full model, $t = 10.0$

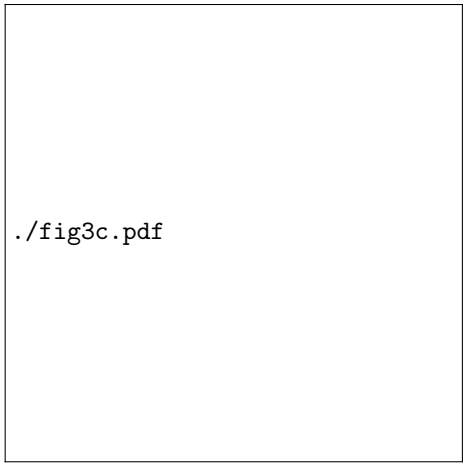

(c) Quadratic expansion, $t = 3.52$

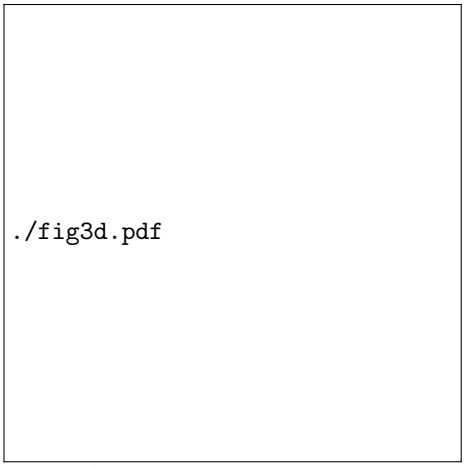

(d) Quadratic expansion, $t = 10.0$

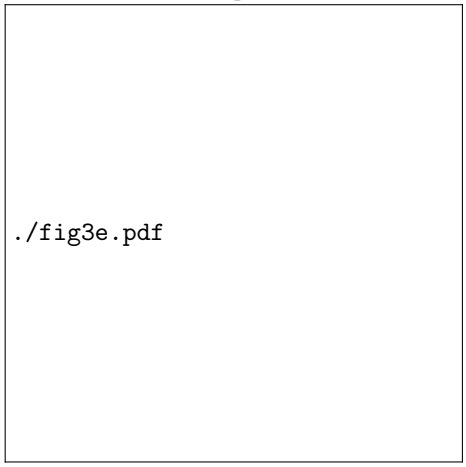

(e) Residual DEIM, $t = 3.52$

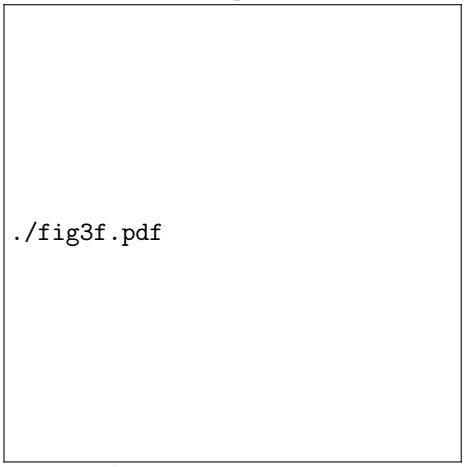

(f) Residual DEIM, $t = 10.0$

Figure 3: These show the solutions of the flow past a cylinder problem at time instances 3.52 and 10.0 seconds. The solutions compare the predictions from the quadratic expansion and residual DEIM models using 48 POD basis functions.

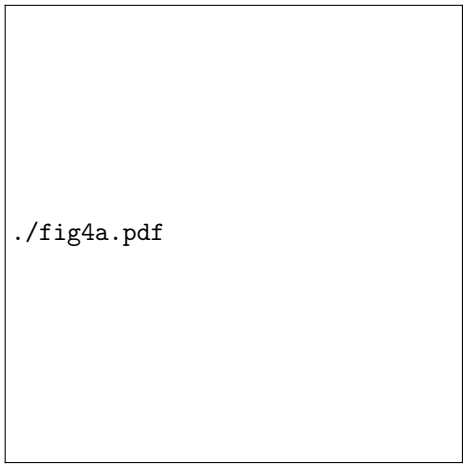

(a) full model, $t = 3.52$

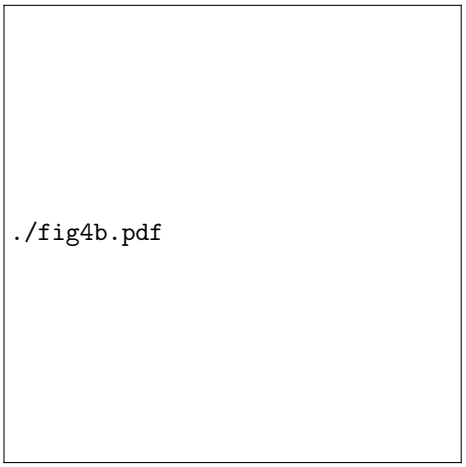

(b) full model, $t = 10.0$

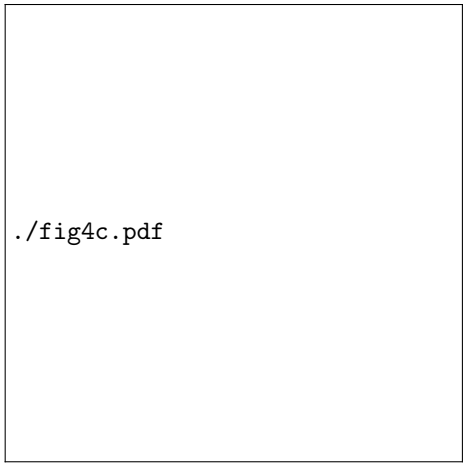

(c) Quadratic expansion, $t = 3.52$

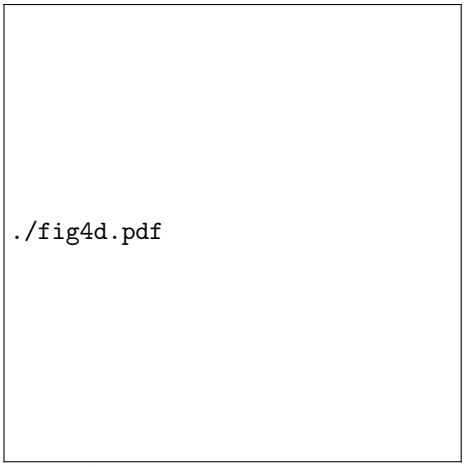

(d) Quadratic expansion, $t = 10.0$

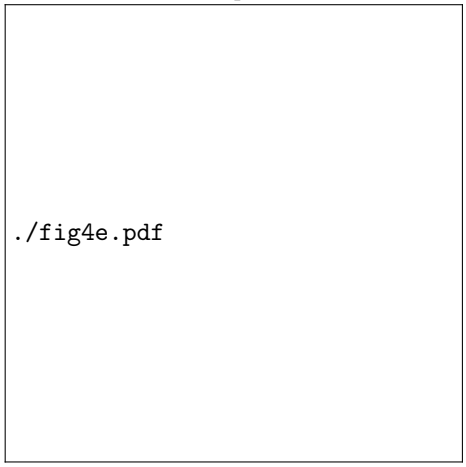

(e) Residual DEIM, $t = 3.52$

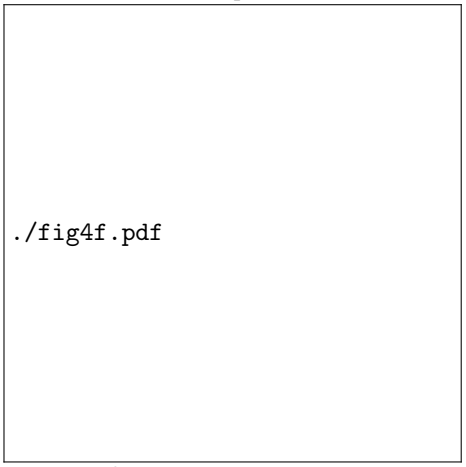

(f) Residual DEIM, $t = 10.0$

Figure 4: These show the solutions of the flow past a cylinder problem at time instances 3.52 and 10.0 seconds. The solutions compare the predictions from the quadratic expansion and residual DEIM models using 96 POD basis functions.

6.2. Case 2: The Gyre problem

The second numerical example involves the simulation of a Gyre for which a circulating fluid moves across a domain that is 1000×1000 km across and 500m in depth. The solution's free surface is driven by a wind with a force strength given by the expression,

$$\tau_y = \tau_0 cos(\pi y/L) \text{ and } \tau_x = 0.0, \tag{68}$$

where L is the problem's length scale given by $L = 1000\ km$. The terms τ_x and τ_y are the wind stresses on the free surface that act along the x and y directions, respectively. In this example the maximum zonal wind stress was set to $\tau_0 = 0.1\ Nm^{-1}$ in the latitude(y) direction. The Coriolis terms are taken into account with the beta-plane approximation(f=βy) where $\beta = 1.8 \times 10^{-11}$ and the reference density of the fluid set to $\rho_0 = 1000\ kgm^{-1}$. With this setup the Reynolds number of the problem was calculated to be $R_e = 250$.

The Gyre was simulated through the full finite element model for a period of 194 days using a time step size of $\Delta t = 0.3311$ days. From this simulation 120 snapshots of the solution and non-linear terms were recorded and from this data 12 POD basis functions were generated. It was found that the POD basis set of this size captured over 99% of the energy of the u, v and p snapshot data. The problem was then re-simulated using the reduced order models with their non-linear terms represented through the quadratic expansion and the residual DEIM methods. Figures 8 presents the velocity profiles obtained through the full model at time instances 91 and 149 days, and these show that the problem has formed several complex flow patterns involving a number of eddies. Included in the figures are the respective solutions obtained through the two reduced order models. Whilst the quadratic expansion method has performed well by resolving the general profile of the solution at these two time instances, some of the finer detail and smaller eddies were not completely captured. These finer solution details were however resolved through the residual DEIM approach. In fact the solutions between the residual DEIM and full model are almost visually identical. The errors between the two reduced models and the full solutions are presented in figure 9. Again these show the residual DEIM method to be more accurate than the quadratic expansion method. It is shown that the main gyre is more accurately resolved using residual DEIM, but in addition the eddies around the central top region of the problem contain less errors.

7. Conclusions

In this article a new reduced order model based upon Proper Orthogonal Decomposition (POD) has been presented. The method is centred on resolving the Navier Stokes equation and the novelty of the approach is in how the non-linear terms of the equations are resolved. The treatment of the non-linear terms within a reduced order model requires special attention since a standard POD approach is no more computationally efficient than a full model solution. Instead additional techniques such as the quadratic expansion method and DEIM have been developed in order to maintain the ROM's efficiency. In this article a new hybrid scheme has been developed that mixes these two approaches. This is based on initially applying the quadratic expansion method to the

non-linear terms and then applying the DEIM approach to resolve the residual between it and the full model. That is, the DEIM is used to mop up the remaining errors left over from the quadratic expansion approach.

This new method, named residual DEIM, has been applied to two 2 dimensional fluid flow problems and compared to the ROM approach using a quadratic expansion. The two problems were based on the simulation of flow past a cylinder and wind driven gyres, both of which were of sufficient difficulty with Reynolds numbers large enough to form complex flow patterns and eddies. In these demonstrations the residual DEIM approach showed strong capabilities in resolving the complex flows efficiently. It was also shown to improve the solution obtained from the ROM model using only quadratic expansions of the non-linear terms. In addition, the reduced order models were developed from full models involving unstructured finite element meshes. It has been previously observed that unstructured meshes can cause stability issues for reduced order models, but this was not the case for the residual DEIM approach. Finally, although no computational times have been stated, the complexity of the residual DEIM is the the same of that of DEIM and the quadratic expansion method. Computational times should therefore be of similar scales to these two previous methods.

Acknowledgments

This work was carried out under funding from the UK's Natural Environment Research Council (projectsNER/A/S/2003/00595,NE/C52101X/1 andNE/C51829X/1), the Engineering and Physical Sciences Research Council (GR/R60898, EP/I00405X/1 and EP/J002011/1), and the Imperial College High Performance Computing Service. Prof. I.M. Navon acknowledges the support of NSF/CMG grant ATM-0931198. Dunhui Xiao acknowledges the support of China Scholarship Council. Andrew Buchan wishes to acknowledge the EPSRC for funding his contribution to this article through the grant ref: EP/J002011/1.

References

[1] K. Fukunaga. Introduction to statistical recognition(2nd edn). *Computer Science and Scientific Computing Series*, Academic Press,Academic Press: Boston, MA.:5–33, 1990.

[2] K. Pearson. On lines and planes of closest fit to systems of points in space. *Philosophical Magazine*, 2:559–572, 1901.

[3] D.T. Crommelin. and A.J. Majda. Strategies for model reduction: Comparing different optimal bases. *Journal of the Atmospheric Sciences*, 61:2206–2217, 2004.

[4] I.T. Jolliffe. Principal component analysis. *Springer, second edition*, pages 559–572, 2002.

[5] Y. Cao, J. Zhu, I.M. Navon, and Z. Luo. A reduced order approach to four dimensional variational data assimilation using proper orthogonal decomposition. *International Journal for Numerical Methods in Fluids*, 53:1571–1583, 2007.

[6] P.T.M. Vermeulen and A.W. Heemink. Model-reduced variational data assimilation. *Monthly Weather Review*, 134:28882899, 2006.

[7] D.N. Daescu and I.M. Navon. A dual-weighted approach to order reduction in 4d-var data assimilation. *Monthly Weather Review*, 136(3):1026–1041, 2008.

[8] X. Chen, F. Fang, and I. M. Navon. A dual weighted trust-region adaptive POD 4D-Var applied to a finite-volume shallow-water equations model. *International Journal for Numerical Methods in Fluids*, 65:520–541, 2011.

[9] X. Chen, S. Akella, and I. M. Navon. A dual weighted trust-region adaptive POD 4D-Var applied to a finite-volume shallow-water equations model on the sphere. *International Journal for Numerical Methods in Fluids*, 68:377–402, 2012.

[10] Muhammad Umer Altaf. *Model Reduced Variational Data Assimilation for Shallow Water Flow Models*. PhD thesis, Delft university of technology, 2011.

[11] J. Du, F. Fang, C.C. Pain, I.M. Navon, J. Zhu, and D.A. Ham. POD reduced-order unstructured mesh modeling applied to 2D and 3D fluid flow. *Computers and Mathematics with Applications*, 65:362–379, 2013.

[12] F.Fang, C.Pain, I.M. Navon, A.H. Elsheikh, J. Du, and D.Xiao. Non-linear Petrov-Galerkin methods for reduced order hyperbolic equations and discontinuous finite element methods. *Journal of Computational Physics*, 234:540–559, 2013.

[13] Pain CC, Piggott MD, Goddard AJH, and et al. Three-dimensional unstructured mesh ocean modelling. *Ocean Modelling*, 10:5–33, 2005.

[14] N.C. Nguyen and J. Peraire. An efficient reduced-order modeling approach for non-linear parametrized partial differential equations. *Int. J. Numer. Meth. Engng.*, 76:27–55, 2008.

[15] M. Barrault, Y. Maday, N.C. Nguyen, and A.T. Patera. An empirical interpolation method: application to efficient reduced-basis discretization of partial differential equations. *C. R. Acad. Sci. Paris, Ser*, 339:667–672, 2004.

[16] Razvan Stefanescu and I.M. Navon. POD/DEIM nonlinear model order reduction of an ADI implicit shallow water equations model. *Journal of Computational Physics*, 237:95–114, 2013.

[17] S. Chaturantabut. Dimension reduction for unsteady nonlinear partial differential equations via empirical interpolation methods. Master's thesis, Rice university, 2008.

[18] S. Chaturantabut and D.C. Sorensen. Nonlinear model reduction via discrete empirical interpolation. *SIAM J. Sci. Comput*, 32:2737–2764, 2010.

[19] S. Chaturantabut and D.C. Sorensen. A state space error estimate for pod-deim nonlinear model reduction. *SIAM Journal on Numerical Analysis*, 50:46–63, 2012.

[20] G Rozza, DBP Huynh, and AT Patera. Reduced basis approximation and a posteriori error estimation for affinely parametrized elliptic coercive partial differential equations- application to transport and continuum mechanics. *Arch Comput Methods Eng*, 15(3):229275, 2008.

[21] NC Nguyen, G Rozza, and AT Patera. Reduced basis approximation and a posteriori error estimation for the time-dependent viscous burgers equation. *Calcolo*, 46(3):157185, 2009.

[22] S Boyaval, C Le Bris, T Lelivre, Y Maday, NC Nguyen, and AT Patera. Reduced basis techniques for stochastic problems. *Arch Comput Methods Eng*, 17(4):435–454, 2010.

[23] JL Eftang, DJ Knezevic, and AT Patera. An hp certified reduced basis method for parametrized parabolic partial differential equations. *Math Comput Model Dyn Syst*, 17(4):395–422, 2011.

[24] D. Xiao, F. Fang, J. Du, C.C. Pain, I.M. Navon*, A. G. Buchan, A.H. ElSheikh, and G. Hu. Non-linear Petrov-Galerkin methods for reduced order modelling of the navier-stokes equations using a mixed finite element pair. *Computer Methods In Applied Mechanics and Engineering*, 255:147–157, 2013.

[25] Baiges, J. Codina, R., and S. Idelsohn. Explicit reduced order models for the stabilized finite element approximation of the incompressible navier-stokes equations. *submitted,Available from cimne.upc.edu*, 2012.

[26] S. Chaturantabut. *Nonlinear Model Reduction via Discrete Empirical Interpolation*. PhD thesis, Rice university, 2011.


./fig5a.pdf


./fig5b.pdf

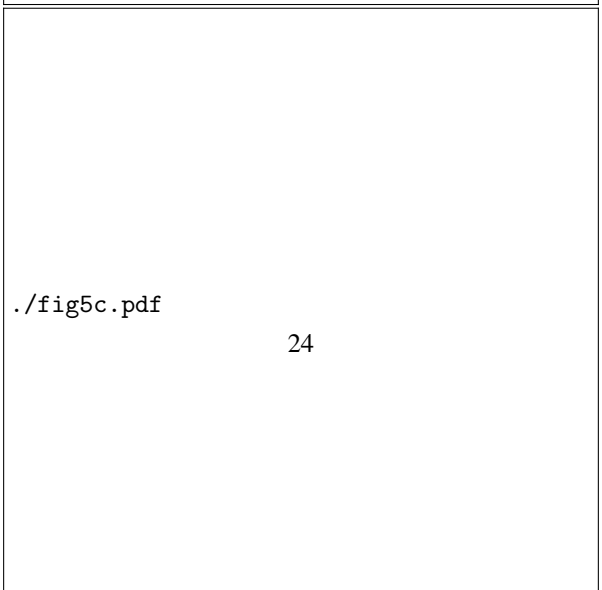
./fig5c.pdf

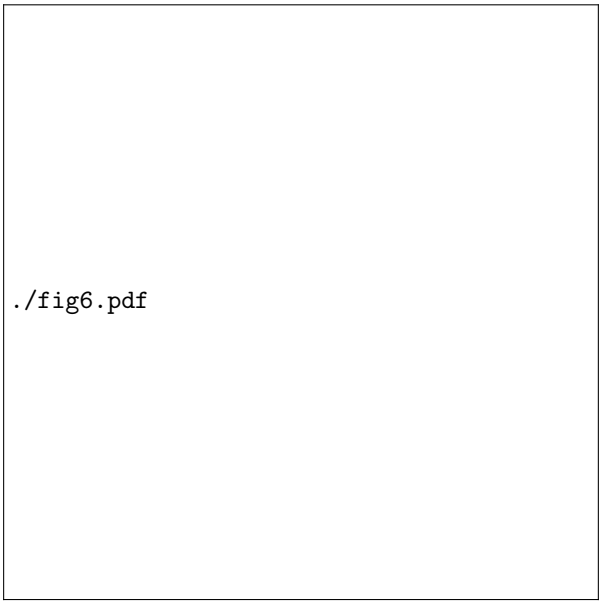

Figure 6: The graph shows the RMSE errors calculated for the quadratic expansion and residual DEIM methods.

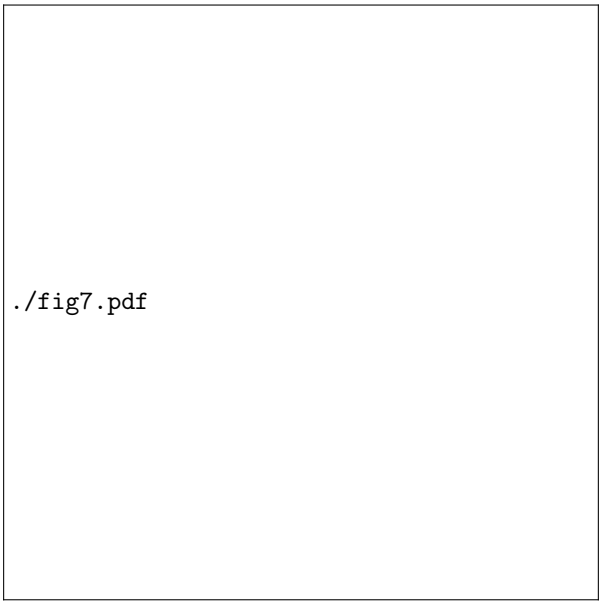

Figure 7: The graph shows the correlation coefficient calculated for the quadratic expansion and residual DEIM methods.

Figure 8: These show the solutions of the gyre problem at time instance 91 (left) and 149 days (right). The solutions compare the predictions from the full model (top), the residual DEIM model (middle) and the quadratic expansion model (bottom). Both reduced order models used 12 POD functions.

Figure 9: These show the solution errors of the gyre problem at time instance 91 (top) and 149 (bottom) days. The solutions compare the errors in the residual DEIM model (left) and the quadratic expansion model (right). Both reduced order models used 12 POD functions.